Improved Arterial Inner Wall Detection Using Generalized Median Computation

Da-Chuan Cheng*[1], Arno Schmidt-Trucksäss[2], Shing-Hong Liu[3], and Xiaoyi Jiang[4]

[1] Department of Radiological Technology, China Medical University, Taiwan
[2] Department of Prevention, Rehabilitation and Sports Medicine, TU München, University Hospital, Germany
[3] Department and Graduate Institute of Computer Science and Information Engineering, Chaoyang University of Technology, Taiwan
[4] Department of Mathematics and Computer Science, University of Münster, Germany

Abstract. In this paper, we propose a novel method for automatic detection of the lumen diameter and intima-media thickness from dynamic B-mode sonographic image sequences with and without plaques. There are two phases in this algorithm. In the first phase a dual dynamic programming (DDP) is applied to detect the far wall IMT and near wall IMT. The general median curves are then calculated. In the second phase, the DDP is applied again using the median curves as the knowledge to obtain a more informed search and to potentially correct errors from the first phase. All results are visually controlled by professional physicians. Based on our experiments, this system can replace the experts' manual work, which is time-consuming and not repeatable.

1 Introduction

Arterial IMT analysis Common carotid artery intima-media thickness (**CCA-IMT**) measurements have been confirmed to be an early marker of atherosclerosis [1] and have been associated with a higher risk of stroke [2] and myocardial infarction [3]. The non-invasive sonographic examination has demonstrated its potential in early predicting cardiovascular diseases. The IMT is an important index in modern medicine and can be measured either manually [4] or automatically [5–11].

Arterial elasticity analysis Moreover, the carotid artery stiffness (**CS**) (or elasticity) is one of the important factors for predicting cardio-vascular (CV) events [12]. The factor CS can be measured via measuring the systolic and diastolic carotid diameter on the distal wall of the CCA, 1 to 2 cm beneath the bifurcation with high-precision sonographic modality. Firstly, carotid distensibility (CDist) is estimated through the variations in arterial cross-sectional area and blood pressure (BP) during systole based on the assumption of a circular lumen. CDist is calculated as CDist=$\Delta A/A \cdot \Delta P$, where A is diastolic lumen area and ΔA is the maximum area change during a systolic-diastolic cycle, and ΔP is the local blood pressure change measured by an applanation tonometer. This pressure change can be approximated by the pressure change measured on the arm in case that the applanation tonometer is deficient. This can be easily done in the routine examination. The CDist can be converted to CS by giving CS=(CDist)$^{-1/2}$ [12].

The automatic methods have the potential in reproducing results and eliminating the strong variations made by manual tracings of different observers. Moreover, the processing time can be considerably reduced. The motivation of this study is to develop a confidential system which is able to detect the intima and adventitia of both near and far artery walls, with or without plaques, automatically even under strong speckle noises using dynamic B-mode sonographic image sequences. This system can identify not only the IMT but also the lumen diameter (**LD**) during systolic and diastolic cycles, from which the artery elasticity can be potentially calculated. Via this system, the dynamic process of carotid artery (**CA**) can be represented by some parameters such as IMT variation, lumen diameter variation, and IMT compression ratio.

This study provides a new technique for detecting the IMT and the LD changes along a section of CCA, which is in general different from previously published works. The proposed system contains two phases. In the first phase, a novel dual dynamic programming (**DDP**) combined with some anatomic knowledge makes the detection more robust against the speckle noises. In the second phase, the generalized median filter is applied and the median curves are calculated, which are fed backwards to the system and the DDP is applied again having the median curves as knowledge to correct its results fully automatically. The proposed scheme has the following steps:

Phase 1:

1. Input image I_k; $1 \leq k \leq K$.
2. If $k = 1$, manually select a rectangle r_1; else, track r_k using knowledge r_1. (Sec.2.3)
3. Extract feature image g_k from I_k having a rectangle r_k. (Sec.2.4)
4. Apply DDP on g_k to detect the dual curves (intima and adventitia). Output c_k^I and c_k^A. (Sec.2.5)
5. Goto Step 1 until $k > K$.

Phase 2:

1. Input c_k^I and c_k^A, $1 \leq k \leq K$, calculate dual median curves M_I and M_A and their corresponding translation t_k^I and t_k^A. (Sec.2.6)
2. Apply DDP onto g_k with guides (M_I, M_A, t_k^I, t_k^A) and output the final intima and adventitia curves for each image I_k; $1 \leq k \leq K$. (Sec.2.7)

The rest part of this paper is organized as follows. In Section 2.1 we address how the image sequences are acquired. The problems of this study are illustrated in Sec. 2.2. The methods are described in Sec. 2.3 to 2.7. Then, results are demonstrated (Sec. 3), discussion and conclusion are given in Sec. 4 and Sec. 5, respectively.

2 Materials and Methods

2.1 Image Acquisition

After at least 15 minutes of rest in the supine position, the ultrasonic examinations of the right and left CCA were performed. An Esaote Mylab 25 ultrasound scanner with a high-resolution and digital beam former was used with a linear variable band 10-13 MHz transducer. The necks of the study subjects were turned slightly to the left or right side. The transducer was positioned at the anterior-lateral side of the neck. The lumen

was maximized in the longitudinal plane with an optimal image of the near and the far vessel wall of the CCA or carotid bifurcation. Thus, typical double lines could be seen as the intima-media layer of the artery. Plaques were scanned in a longitudinal and cross-sectional plane showing the highest diameter. At least two heart cycles of every subject were acquired for measurement of the IMT or plaque, respectively. All sequences were stored digitally in the ultrasound device and transferred to a commercially available computer for further image analysis.

2.2 Problem statement

Figure 1 shows a typical image made by our sonographic modality. The **first** problem is the impact of speckle noises. It is very common that there are speckle noises in the artery lumen. In general, the noises on the near-wall side are stronger than the noises on the far-wall side. It makes the detection of near wall intima much more difficult, comparing to the detection of far wall intima. **Second**, some diseases such as atherosclerotic plaques change the structure of IM complex or the intimal layer. Some changes result in strong echoes such as calcification. When the intima is damaged, there are nearly no echoes on the damaged part. In this case, the adventitia might be exposed on the artery lumen. **Third**, we found the plaque might cause in different echoes in the same places in the dynamic B-mode sonography, which might cause ambiguity in adventitia recognition. This problem is indicated in Fig.1(b), (c), and Fig.2(h). There is an echo near the adventitia, which is absent on the most images. The DDP detects it because it does exist some echoes. However, according to the human beings judgment, since the majority has no such echo so the majority wins. This detection as shown in Fig.1(b) and (c) would be judged to be false. **Finally**, the target we are processing is moving during the image sequence since it is made by dynamic B-mode sonography. Therefore we have to deal with the tracking problem. Fortunately, the target we are tracking does not change its shape in a large scale. We assume that the artery movement is only in longitudinal direction, although there is less movement in horizontal direction. This movement is due to the systolic and diastolic cycle. Moreover, there is no overlapping or shadow problems, which might happen very often in the camera videos. In order to conquer problems listed above, we propose the novel scheme as follows.

(a) (b) (c)

Fig. 1. A typical B-mode sonographic image. (a) A sub-image from a dynamic image sequence. (b) The DDP result superimposed on the sub-image of Frame No. 43. (c) The DDP result on Frame No. 45.

2.3 Artery movement tracking

Since the artery is moving during heart cycles in the dynamic B-mode sonography, the artery tracking is an important issue. It is assumed that the artery has 1D movement, i.e., in the vertical direction. This movement is actually an extension of the artery lumen in the heart systolic cycle. In addition, the whole artery might have a shift in the vertical direction in a whole heart cycle. This system needs only one single manual input in the beginning. The user has to select a rectangle area to cover the section area to be measured. However, the artery might move out of this given rectangle in the subsequent images. Therefore, a simple automated tracking algorithm is combined to help the system finding the correct artery position in each image. Due to page limitation, details are omitted here and the readers are referred to [13].

2.4 Image Features

The objective of this study is to detect the intima, adventitia of CA, and plaque outline if any. There are many kinds of methods achieving the same goal. Some used gray level or the gradient of gray level as features [7, 11, 6]. In this study, we use a simple feature extraction method which is able to detect the intima and adventitia of both near and far wall as well as plaques of CCA in dynamic B-mode sonography [11, 14, 13]. Here we do not repeat the feature extraction process.

2.5 Dual dynamic programming (DDP)

In our previous study [11] we have developed dual dynamic programming (DDP) for IMT detection. Some following works are based on this method which are able to detect the IMT and the lumen diameters [14, 13]. Let $g_k(x, y)$ denote the k-th feature image grid of size $M \times N$, where M and N are the number of rows and columns, respectively. Assume the DDP running from left to right in order to find dual curves intima and adventitia of the far wall. The DDP intends to find the global maximum, which is the summation of the feature values on the grid where the dual curves go through. The dual curves can be denoted as a point set $\{(i, y1_i), (i, y2_i)\}, 1 \leq i \leq N$, and its corresponding feature values are $\{g_k(i, y1_i),\ g_k(i, y2_i)\}$. The cost function finding the k-th dual curves can finally be defined as:

$$
\begin{aligned}
J_i(y_1, y_2) = \min_{\substack{j_1, j_2 \in \\ \{-d_r, \cdots, d_r\}}} & \{J_{i-1}(y_1 + j_1, y_2 + j_2) + g_k(i, y_1) \\
& + g_k(i, y_2) + \lambda_1 |w_i - w_{i-1}| + \lambda_2 (|j_1| + |j_2|))\} \\
& \text{subject to } d_{min} \leq y_1 + j_1 - y_2 - j_2 \leq d_{max}, \\
& d_r \leq |y_{1i} - y_{1\ i-1}|,\ d_r \leq |y_{2i} - y_{2\ i-1}| \text{ and } 2 \leq i \leq N.
\end{aligned} \tag{1}
$$

where λ_1 and λ_2 are weighting factors of the curve smoothness. The parameters y_1, y_2 are the short form of y_{1i}, y_{2i}, respectively. All tuples (y_1, y_2) are tested if they fit the constraint given in Eq.(1). The following steps including the initialisation and backwards tracing the dual paths can be found in [13]. The output (y_1^*, y_2^*) which satisfies the global maximization is then redefined to (y_k^A, y_k^I) for following steps.

2.6 Generalized median filter

In this section, we address a clinical application of generalized median filter [15] to produce a median curve representing either detected intimal or adventitial curve. Suppose we have a sequence having K images, from each image the intimal layer is detected and represented by c_k^I, where $k = 1, 2, \cdots, K$ denotes the k-th image. Since the curve goes from left to right, the x-coordinate is in an ascending order. The important information is the y-coordinate which is represented by y_k^I of the corresponding curve c_k^I. The goal is to find a generalized median curve M_I which has the minimum error to all these detected curves c_k^I. However, since the artery has movement because the heart cycle, there is another parameter t_k^I representing the translation of the corresponding intimal curve on the k-th image. Therefore, the cost function to find out the generalized median curve of intima is defined as follows:

$$f(M_I, T_I) = \sum_{k=1}^{K} \sum_{i=1}^{N} (y_{ki}^I - y_i^I - t_k^I)^2 \tag{2}$$

where
$M_I = \{y_i^I | 1 \leq i \leq N\}$ is the median curve, N is the curve length;
y_k^I is the y-coordinate of the k-th curve c_k^I which has n points;
$T_I = \{t_k^I | 1 \leq k \leq K\}$ is the composition of all translations for each curve c_k^I.
Through some derivations, one can easily obtain:

$$t_k^I = \frac{1}{N} \sum_{i=1}^{N} (y_{ki}^I - y_i^I) \tag{3}$$

$$y_i^I = \frac{1}{K} \sum_{k=1}^{K} (y_{ki}^I - t_k^I) \tag{4}$$

which can be solved iteratively by an EM algorithm. The calculations of $M_A = \{y_i^A | 1 \leq i \leq N\}$ and T_A for adventitia are similar.

2.7 Dual dynamic programming with guides

Here we briefly describe how DDP uses median curves as guides. Let $g_k(x, y)$ denote the k-th feature image grid as defined in Sec.2.5.

The anatomic knowledge ($y_1 > y_2$, d_{min}, and d_{max}), the guides by the median curves (y^I for intima and y^A for adventitia) and the translations t_k^I and t_k^A are then embedded into the DDP structure. The cost function finding the k-th dual curves can finally be defined as:

$$\begin{aligned} J_i(y_1, y_2 | y^I, y^A, t_k^I, t_k^A) = \min_{\substack{j_1, j_2 \in \\ \{-d_r, \cdots, d_r\}}} \{ & J_{i-1}(y_1 + j_1, y_2 + j_2 | y^I, y^A, t_k^I, t_k^A) + g_k(i, y_1) \\ & + g_k(i, y_2) + \lambda_1 |w_i - w_{i-1}| + \lambda_2 (|j_1| + |j_2|) + \lambda_3 (|y_1 + j_1 - (y^A - t_k^A)| \\ & + |y_2 + j_2 - (y^I - t_k^I)|)\} \\ & \text{subject to } d_{min} \leq y_1 + j_1 - y_2 - j_2 \leq d_{max}, \\ & d_r \leq |y_{1i} - y_{1\ i-1}|,\ d_r \leq |y_{2i} - y_{2\ i-1}|, \text{ and } 2 \leq i \leq N. \end{aligned} \tag{5}$$

where λ_1 and λ_2 are weighting factors of the curve smoothness; λ_3 is the weighting for median curves. The parameters y_1, y_2, y^A, and y^I are the short form of y_{1i}, y_{2i}, y_i^A, and y_i^I, respectively. All tuples (y_1, y_2) are tested if they fit the constraint given in Eq.(5). The following steps including the initialisation and backwards tracing the dual paths can be found in [13]. The output (y_1^*, y_2^*) which satisfies the global maximization are the adventitia and intima of the corresponding k-th image.

3 Results

Figure 2 demonstrates the IMT and a plaque detection on the far wall. The problem we want to solve in this paper is indicated in Fig. 2(h). There is an echo existing near adventitia in the frames from frame number 40 to 46. We illustrate only frame number 41 and 44 as examples. With single DDP it can detect the adventitia as shown in the second column. However, these results are judged to be wrong by an experienced physician. This is because in the rest frames there existed no such an echo, which are in majority. The generalized median filter uses the property that the majority wins so that it can simulate human beings judgment. It obtains the correct results as shown in the third column. Due to page limitation, all results cannot be displayed here. However, the results made by single DDP are similar to Fig.2(e) and (h) from frame No. 40 to 46. The results made by this proposed scheme are similar to Fig.2(f) and (i) from frame No. 40 to 46 as shown in Fig.3.

4 Discussion

The programs are setup on the Matlab platform. Some kernel functions are written in C to speedup the whole process. The parameters used in this paper are: $d_r = 1$, $d_{min} = 4$ in IMT detection, $d_{min} = 20$ in LD detection, $d_{max} = 40$ in IMT detection, $d_{max} = 0.9 \cdot M$ in LD detection, and $\lambda_1 = \lambda_2 = 0.1$, and $\lambda_3 = 0.05$. The computer has Intel Core(TM)2 T5600 CPU with 1.83GHz, 2GB RAM. The computation time for IMT detection is around 1.2 sec for the DDP with guides.

The novel system is able to detect the near and far wall IMT and the lumen diameter of CCA in the B-mode sonographic videos, with and without plaques. Having these results, we can provide physicians the CCA diameter changes during the heart cycle, the compression rate of IMT, the plaque thickness and shape morphology. Furthermore, in the future we are able to build the blood flow model to predict the shear stress on the artery wall, which is a critical index for the vascular diseases.

5 Conclusion

In this paper we propose an intelligent method to detect the near and far wall IMT as well as the LD of CCA in dynamic B-mode sonography, with and without plaques. Based on the experiments, the detection results are correct and do not need any manual correction. This system is fully automated except it needs an initial rectangle area selected by the user. In the future work, we will explore the relationship between some diseases and the parameters extracted from the dynamic IMT and LD by our system.

6 Acknowledgment

This work is supported by the National Science Council (NSC), Taiwan, under Grant NSC 97-2218-E-039-001.

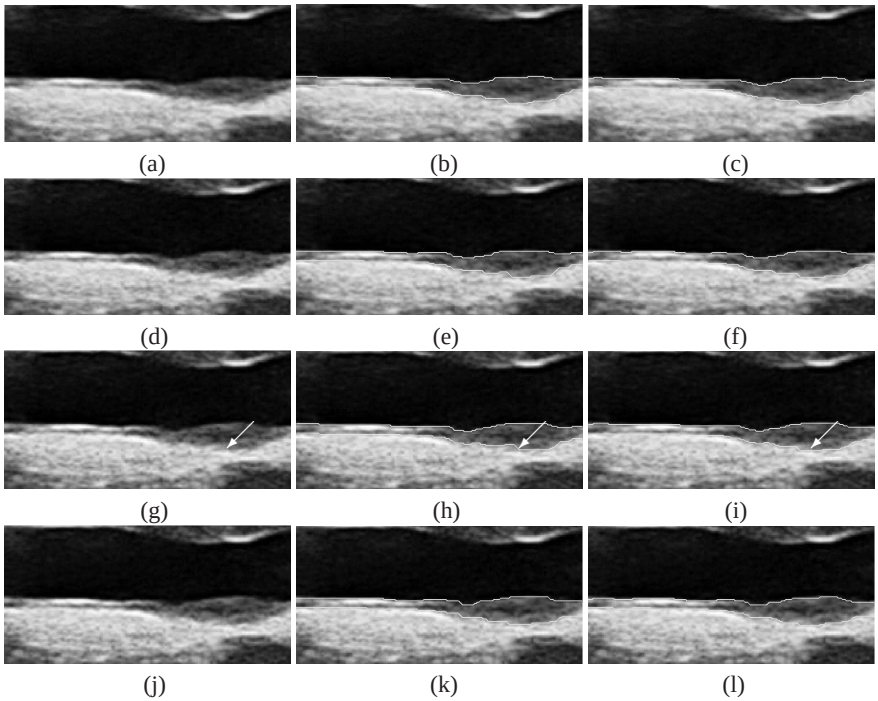

Fig. 2. The far wall IMT and plaque detection: The first column are the raw sub-images; they are frame No. 38, 41, 44, and 47, respectively. The second column are the results of DDP superimposed on the raw sub-images. The third column are the results of proposed scheme superimposed on the raw sub-images.

References

1. Bonithon Kopp, C., Scarabin, P., Taquet, A., Touboul, P., Malmejac, A., Guize, L.: Risk factors for early carotid atherosclerosis in middle-aged french women. Arterioscler Thromb. **11** (1991) 966–972
2. O'Leary, D., Polak, J., Kronmal, R., Manolio, T., Burke, G., Wolfson, S.J.: Carotid-artery intima and media thickness as a risk factor for myocardial infarction and stroke in older adults. N Engl J Med **340** (1999) 14–22
3. Bots, M., Grobbee, D., Hofman, A., Witteman, J.: Common carotid intima-media thickness and risk of acute myocardial infarction. the role of lumen diameter. Stroke **36** (2005) 762–767
4. Vemmos, K., Tsivgoulis, G., Spengos, K., Papamichael, C., Zakopoulos, N., Daffertshofer, M., Lekakis, J., Mavrikakis, M.: Common carotid artery intima-media thickness in patients with brain infarction and intracerebral haemorrhage. Cerebrovascular Diseases **17** (2004) 280–286
5. Touboul, P., Elbaz, A., C.Koller, Lucas, C., Adrai, V., Chédru, F., P.Amarenco: Common carotid artery intima-media thickness and brain infarction, the étude du profil génétique de l'infarctus cérébral (génic), case-control study. Circulation **102** (2000) 313–318

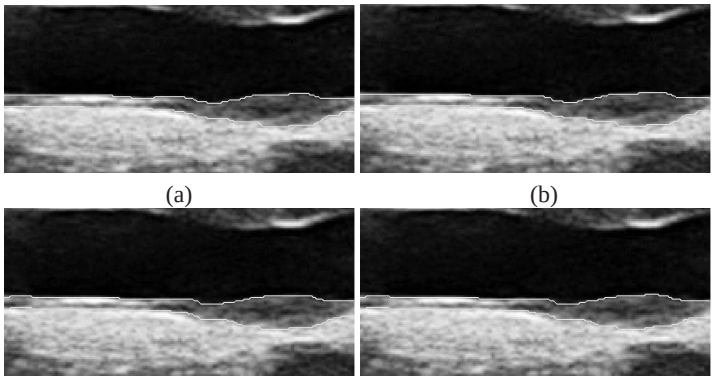

Fig. 3. Results of proposed method: From (a)-(d) are Frame No. 42, 43, 45, and 46.

6. Liang, Q., Wendelhag, I., Wikstrand, J., Gustavsson, T.: A multiscale dynamic programming procedure for boundary detection in ultrasonic artery images. IEEE Trans. on Medical Imaging **19** (2000) 127–142
7. Cheng, D., Schmidt-Trucksäss, A., Cheng, K., Burkhardt, H.: Using snakes to detect the intimal and adventitial layers of the common carotid artery wall in sonographic images. Computer Methods and Programs in Biomedicine **67** (2002) 27–37
8. Kanai, H., Hasegawa, H., Ichiki, M., Tezuka, F., Koiwa, Y.: Elasticity imaging of atheroma with transcutaneous ultrasound: Preliminary study. Circulation **107** (2003) 3018–3021
9. Hasegawa, H., Kanai, H., Koiwa, Y.: Detection of lumen-intima interface of posterior wall for measurement of elasticity of the human carotid artery. IEEE Trans. on Ultrasonics Ferroelectrics & Frequency Control **51**(1) (2004) 93–109
10. Cardinal, M.H.R., Meunier, J., Soulez, G., Maurice, R., É. Therasse, Cloutier, G.: Intravascular ultrasound image segmentation: A three-dimensional fast-marching method based on gray level distributions. IEEE Trans. on Medical Imaging **25**(5) (2006) 590–601
11. Cheng, D.C., Jiang, X.: Detections of arterial wall in sonographic artery images using dual dynamic programming. IEEE Trans. on Information Technology in Biomedicine **12**(6) (2008) 792–799
12. Paini, A., Boutouyrie, P., Calvet, D., Tropeano, A.I., Laloux, B., Laurent, S.: Carotid and aortic stiffness: Determinants of discrepancies. Hypertension **DOI: 10.1161/01.HYP.0000202052.25238.68** (2006)
13. Cheng, D.C., Schmidt-Trucksäess, A., Pu, Q., Liu, S.H.: Motion analysis for artery lumen diameter and intima-media thickness of carotid artery on dynamic B-mode sonography. In: International Conference on Mass-Data Analysis of Images and Signals in Medicine, Biotechnoogy, Chemistry and Food Industry. (July 2009) Accepted
14. Cheng, D.C., Pu, Q., Schmidt-Trucksäess, A., Liu, C.H.: A novel method in detecting CCA lumen diameter and IMT in dynamic B-mode sonography. In: The 13th International Conference on Biomedical Engineering. (December 2008) 734–737
15. Wattuya, P., Jiang, X.: A class of generalized median contour problem with exact solution. In: Proc. of 11th Int. Workshop on Structural Pattern Recognition, Hong Kong (2006)